

On the eigenmodes of compact hyperbolic 3-manifolds

Neil J. Cornish & David N. Spergel

Department of Astrophysical Sciences, Peyton hall, Princeton University, Princeton, NJ 08544-1001, USA

We present a simple algorithm for finding eigenmodes of the Laplacian for arbitrary compact hyperbolic 3-manifolds. We apply our algorithm to a sample of twelve manifolds and generate a list of the lowest eigenvalues. We also display a selection of eigenmodes taken from the Weeks space.

Eigenmodes of the Laplace operator contain a wealth of information about the geometry and topology of a manifold. This is especially true for hyperbolic 3-manifolds, where the Mostow-Prasad rigidity theorem [1] ensures that distinct manifolds have distinct eigenvalue spectra: To echo the words of Marc Kac [2], one can “hear the shape” of a hyperbolic drum.

Unfortunately, the eigenmodes of a compact hyperbolic 3-manifold (CHM) cannot be expressed in closed analytic form, so numerical solutions must be sought. A variety of numerical methods exist to solve the problem, including variational principles based on the finite element method [3]. Perhaps the most powerful method is the boundary element method developed by Aurich and Steiner [4]. Here we present an alternative method that came out of our work on multi-connected cosmological models [5,6]. While technically inferior to the boundary element method, our approach is better suited to studying a large sample of manifolds since the only inputs are the group generators. In contrast, the boundary element method requires some human effort prior to each numerical evaluation. To-date, the boundary element method has only been applied to two 3-dimensional examples, a tetrahedral orbifold [7], and the Thurston manifold [8]. Consequently, the majority of the eigenvalue spectra described in this paper are completely new.

I. PRELIMINARIES

We seek to solve the eigenvalue problem

$$-\Delta\Psi_q = q^2\Psi_q, \quad (1.1)$$

for compact hyperbolic 3-manifolds $\Sigma = H^3/\Gamma$, where the fundamental group, Γ , is a discrete subgroup of $SO(3,1) \cong PSL(2,C)$ acting freely and discontinuously. The metric on the universal cover H^3 can be written in spherical coordinates (ρ, θ, ϕ) :

$$ds^2 = d\rho^2 + \sinh^2 \rho (d\theta^2 + \sin^2 \theta d\phi^2). \quad (1.2)$$

In these coordinates the Laplace operator acting on a scalar function Ψ takes the form

$$\Delta\Psi = \frac{1}{\sinh^2 \rho} \left[\frac{\partial}{\partial \rho} \left(\sinh^2 \rho \frac{\partial \Psi}{\partial \rho} \right) + \frac{1}{\sin^2 \theta} \frac{\partial}{\partial \theta} \left(\sin \theta \frac{\partial \Psi}{\partial \theta} \right) + \frac{1}{\sin^2 \theta} \frac{\partial^2 \Psi}{\partial \theta^2} \right]. \quad (1.3)$$

In the simply connected space H^3 , the eigenvalues take all values in the range $q^2 = [1, \infty)$, and the eigenmodes are given by

$$Q_{q\ell m}(\rho, \theta, \phi) = X_q^\ell(\rho) Y_{\ell m}(\theta, \phi). \quad (1.4)$$

Here the $Y_{\ell m}$'s are spherical harmonics and the radial eigenfunctions are given by the hyperspherical Bessel functions

$$X_q^\ell(\rho) = \frac{(-1)^{\ell+1} \sinh^\ell \rho}{\left(\prod_{n=0}^{\ell} (n^2 + k^2) \right)^{1/2}} \frac{d^{\ell+1} \cos(k\rho)}{d(\cosh \rho)^{\ell+1}}. \quad (1.5)$$

The wavenumber, k , is related to the eigenvalues of the Laplacian by

$$k^2 = q^2 - 1. \quad (1.6)$$

The modes have wavelength $\lambda = 2\pi/k$ and an amplitude that decays as $1/\sinh(\rho)$. The eigenmodes satisfy the delta-function normalization

$$\int_0^\infty \int_0^\pi \int_0^{2\pi} \sinh^2 \rho d\rho \sin \theta d\theta d\phi (Q_{q\ell m} Q_{q'\ell'm'}^*) = \delta(q - q') \delta_{\ell\ell'} \delta_{mm'}. \quad (1.7)$$

In principle, the eigenmodes in the multi-connected, compact space Σ can be lifted to the universal cover and expressed in terms of the eigenmodes of H^3 :

$$\Psi_q = \sum_{\ell=0}^{\infty} \sum_{m=-\ell}^{\ell} a_{q\ell m} Q_{q\ell m}. \quad (1.8)$$

The modes Ψ_q must satisfy the property

$$\Psi_q(x) = \Psi_q(gx) \quad \forall g \in \Gamma \text{ and } \forall x \in H^3, \quad (1.9)$$

which places restrictions on the expansion coefficients $a_{q\ell m}$. Indeed, it will only be possible to satisfy (1.9) when q^2 is an eigenvalue of the compact space. To find the eigenmodes we numerically solve (1.9) using a singular value decomposition.

II. THE NUMERICAL METHOD

Our approach to solving (1.9) is completely straightforward. We begin by randomly selecting a collection of

d points inside the Dirichlet domain. Taking the face-pairing generators g_α of Γ , we find all images of our collection of points out to some distance ρ_{\max} in the covering space. How we chose this distance will be explained later. Each point p_j yields n_j images and $n_j(n_j + 1)/2$ equations of the form

$$\Psi(g_\alpha p_j) - \Psi(g_\beta p_j) = 0, \quad (\alpha \neq \beta). \quad (2.1)$$

At each point $x = g_\alpha p_j$ the function $\Psi(x)$ is decomposed into eigenmodes of the covering space with wavenumber k :

$$\Psi_k(x) = \sum_{\ell=0}^L \sum_{m=-\ell}^{\ell} a_{k\ell m} Q_{k\ell m}(x). \quad (2.2)$$

How we choose L will be explained in due course. Finding the $Q_{k\ell m}$'s at each point is easy as there exist numerically stable recursion relations for both the hyper-spherical Bessel functions and the spherical harmonics. Schematically, we arrive at the system of equations

$$\begin{array}{c} \uparrow \\ M \\ \downarrow \end{array} \left[\begin{array}{ccc} (Q_{00}(g_1 p_1) - Q_{00}(g_2 p_1)) & \cdots & (Q_{LL}(g_\alpha p_1) - Q_{LL}(g_\beta p_1)) \\ \vdots & \ddots & \vdots \\ (Q_{00}(g_1 p_d) - Q_{00}(g_2 p_d)) & \cdots & (Q_{LL}(g_\alpha p_d) - Q_{LL}(g_\beta p_d)) \end{array} \right] \begin{array}{c} \left[\begin{array}{c} a_{00} \\ \vdots \\ a_{LL} \end{array} \right] \\ = \\ \left[\begin{array}{c} 0 \\ \vdots \\ 0 \end{array} \right] \end{array}. \quad (2.3)$$

$\leftarrow \qquad \qquad \qquad N \qquad \qquad \qquad \rightarrow$

The number of rows, M , is equal to

$$M = \sum_{j=1}^d n_j(n_j + 1)/2, \quad (2.4)$$

and the number of columns, N , is equal to

$$N = \sum_{\ell=0}^L \sum_{m=-L}^L 1 = (L + 1)^2. \quad (2.5)$$

To fix the $a_{k\ell m}$'s up to an overall normalization requires M to equal $N - 1$. When $M = N - 1$, a solution exists for any k . However, if $M > N$ a solution only exists when k corresponds to an eigenvalue of the compact space. The standard numerical method for solving over-constrained systems of equations is the Singular Value Decomposition (SVD) [9]. For a system of the form

$$\overline{\overline{A}} \cdot \overline{a} = \overline{0}, \quad (2.6)$$

the SVD returns solution vectors \overline{a} that minimize

$$\chi^2 = \left| \overline{\overline{A}} \cdot \overline{a} \right|^2. \quad (2.7)$$

By incrementing in k , the eigenvalues are revealed by minima in the function $\chi^2(k)$. Eigenmodes with multiplicity greater than unity will yield multiple solution vectors \overline{a} .

All that remains to be done is to decide on optimal choices for $L = \ell_{\max}$, the tiling radius ρ_{\max} and the degree of over-constraint $c = M/N$. The choice of L and

ρ_{\max} is dictated by the structure of the radial eigenfunctions $X_k^\ell(\rho)$. In broad outline, they are of the form

$$X_k^\ell(\rho) \approx \begin{cases} 0 & \rho \ll \rho_0 \\ \frac{\cos(k\rho + \phi_0)}{\sinh(\rho)} & \rho \gg \rho_0. \end{cases} \quad (2.8)$$

The constants ϕ_0 and ρ_0 depend on k and ℓ . For fixed k , ρ_0 increases monotonically with increasing ℓ . Therefore, if we restrict our attention to some finite region with $\rho \leq \rho_0$, we need only consider a finite number of multipoles L . With ℓ held fixed, ρ_0 decreases monotonically with increasing k . Thus, if we hold $\rho_{\max} \approx \rho_0$ fixed, we must increase L as k increases. Alternatively, if we hold L fixed, we must decrease ρ_{\max} as k increases.

Because the number of computational steps scales as L^6 , it makes sense to keep L as small as possible. However, small values of L yield small values of ρ_0 , which

in turn limits the number of images we are able to collect for each point. As a compromise, we choose L to be as small as possible, while leaving ρ_{\max} large enough for there to be at least 10 images of each point. Numerically we set ρ_{\max} to be the first solution to the transcendental equation

$$X_k^L(\rho) \sinh(\rho) = 0.25. \quad (2.9)$$

We also found it advantageous to fix a minimum radius in the same way, but with L replaced by ℓ_{\min} in the above equation. The inner cut-off helps to keep the $Q_{k\ell m}$'s of similar size. Finally, we found the optimal degree of over-sampling to lie in the range $10 \rightarrow 100$, with the high end of the range being required at low k and L . At higher k the radial eigenfunctions look less alike and a lower over-sampling can be used. Good all purpose choices covering the range $k = 1$ to $k = 20$ are:

$$\begin{aligned} L &= 10 + [k], \\ \ell_{\min} &= 5, \\ c &= 10 + [100/k], \end{aligned} \quad (2.10)$$

though the algorithm performs well for a wide range of inputs. The eigenmodes derived using the above choice of inputs are good to within a few percent. Choosing L and c larger improves the eigenmodes, but at the cost of slowing down the computations.

The SVD returns solution vectors for the $a_{k\ell m}$ normalized such that

$$\sum_{\ell=0}^L \sum_{m=-\ell}^{\ell} |a_{k\ell m}|^2 = 1. \quad (2.11)$$

Thus, the eigenmodes are automatically delta-function normalized in H^3 . To normalize the modes in the compact space Σ we numerically perform the integral

$$\int_{\Sigma} \Psi_k(x) \Psi_{k'}^*(x) dV. \quad (2.12)$$

When $k = k'$ we normalize to one, and when $k \neq k'$ we check that the integral vanishes (or is at least tolerably small).

A. Example

We begin by choosing an example from Jeff Weeks' *SnapPea* [10] census of closed hyperbolic 3-manifolds and ask *SnapPea* for the face-pairing generators. Taking $m188(-1,1)$ as a randomly chosen example, we ran our code out to $k = 10$ to produce the $\chi^2(k)$ shown in Fig. 1. The χ^2 's for the five best solution vectors are shown. The eigenvalues appear as clear minima in the χ^2 of the best fit solution vector. The first mode to have multiplicity greater than one occurs at $k = 8.34$. However, below $k = 8$ we see that the χ^2 of the second best solution vector occasionally exhibits minima at local maxima of the best fit solution vector. This occurs when the second best fit is formed from a weighted superposition of adjacent eigenmodes. In contrast, when an eigenmode has multiplicity greater than one the minima of the second best fit coincides with that of the best fit. This behaviour is due to the SVD returning an orthonormal set of solution vectors.

When successive minima are close together, such as occurs near $k = 9.8$ in Fig. 1, care must be taken in locating successive minima as they can be displaced from their true positions. This problem is a familiar one for astronomers who study spectral lines in starlight, and we were able to use the same deconvolution techniques to study our eigenspectra. The results of our analysis are compiled in Table I, where the eigenvalues and their multiplicities are recorded.

TABLE I. Eigenvalue spectrum, q^2 , for $m188(-1,1)$.

20.4	22.6	27.2	30.2	39.6	46.2
1	1	1	1	1	1
51.8	55.3	60.1	70.6	75.5	78.8
1	1	1	2	2	1
80.9	83.1	86.0	96.8	98.0	99.4
1	1	1	2	1	1

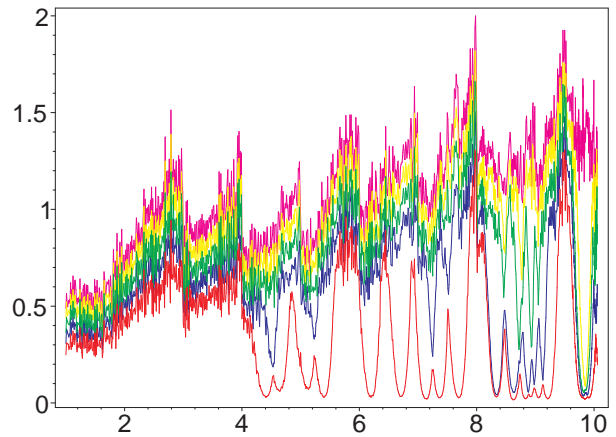


FIG. 1. The χ^2 spectrum for $m188(-1,1)$ in the range $k = 1 \rightarrow 10$.

III. RESULTS AND CHECKS

We applied a battery of tests to our results. The first was to reproduce Inoue's [8] results for the Thurston manifold. Calling up $m003(-2,3)$ from the *SnapPea* census, we generated the collection of low-lying eigenmodes recorded in Table II.

Inoue was able to generate modes with $q^2 \leq 100$, and in this range our eigenvalues agree. However, we discovered that Inoue had missed eigenmodes at $q^2 = 46.2$ and $q^2 = 59.1$. Past $q^2 = 100$ we are in uncharted territory, so other checks have to be applied. One simple check is to compare the spectral staircase, *i.e.* the number of modes with wavenumber $\leq k$, with the prediction of Weyl's asymptotic formula

$$N(\leq k) \asymp \frac{\text{Vol}(\Sigma)}{6\pi^2} k^3 + \text{const.} \quad (3.1)$$

TABLE II. Eigenvalue spectrum for the Thurston space.

29.3	33.5	46.2	47.8	50.8	59.1
1	1	2	1	1	2
68.9	73.8	76.2	85.8	95.1	98.0
1	1	1	2	1	1
100.1	107.5	113.8	115.5	117.4	123.3
1	1	1	2	1	2
130.3	137.9	140.0	144.5	149.8	156.3
1	2	1	2	1	1
160.5	164.1	166.6	169.5	175.0	178.2
1	2	2	1	1	1
184.6	192.3	197.8	204.3	207.2	209.8
2	2	4	2	1	1

From Fig. 2 we see that the spectral staircase closely follows the Weyl formula. Another check we applied to the eigenmodes was to evaluate the integral (2.12) for modes with unequal k . The typical overlap was found to be on the order of a few percent, which is comparable to the performance of the boundary element method.

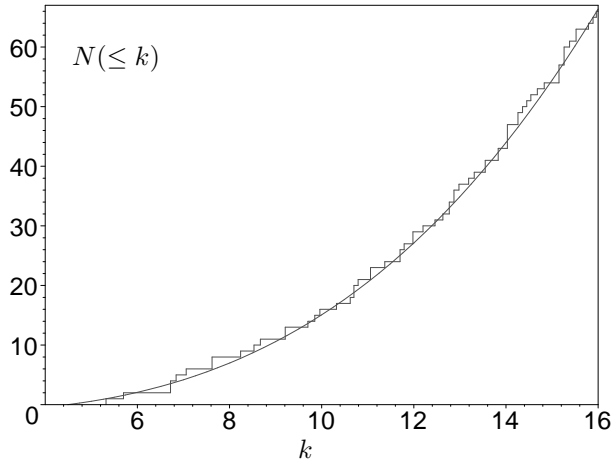


FIG. 2. The spectra staircase for $m003(-2, 3)$ showing its convergence toward the Weyl asymptotic formula.

A. The Weeks Space

To really put our code to the test we decided to study the Weeks space. This space has the distinction of being the smallest known hyperbolic 3-manifold, and is now generally thought to be *the* smallest example. The Weeks space provides a challenge to eigenmode solvers as it has an unusually large symmetry group. Consequently, many of the modes will be highly degenerate. The symmetry group is the Dihedral group of order 6, which has the presentation

$$D_6 = \langle a, b \mid a^6, b^2, ba^{-1}ba^{-1} \rangle. \quad (3.2)$$

The geometrical interpretation is that there exists a closed geodesic about which the space has a six-fold rotational symmetry, and a second closed geodesic, orthogonal to the first, about which the manifold has a reflection symmetry. If we were to choose the basepoint of our Dirichlet domain at one of the points where the two geodesics intersect, the resulting fundamental polyhedron would enjoy the full D_6 symmetry*. Because of the D_6 symmetry, we expect to find modes with 1, 2, 3, 4 and 6 fold degeneracy.

*We thank Jeff Weeks and Craig Hodgson for providing us with this description.

Taking the Weeks space $m003(-3, 1)$ from the *SnapPea* census, we located the first 74 eigenmodes. These are listed in Table III along with their multiplicities. Many of the higher eigenmodes are highly degenerate, in keeping with our expectations. The spectral staircase shown in Fig. 3 is in excellent agreement with Weyl’s asymptotic formula.

For those curious to see what the eigenmodes themselves look like, we display a series of slices through a selection of modes. These appear in Figures 5 and 6. For reference we also display a view of the Dirichlet domain in Fig. 4, to help make contact with the 3-dimensional structure of the modes.

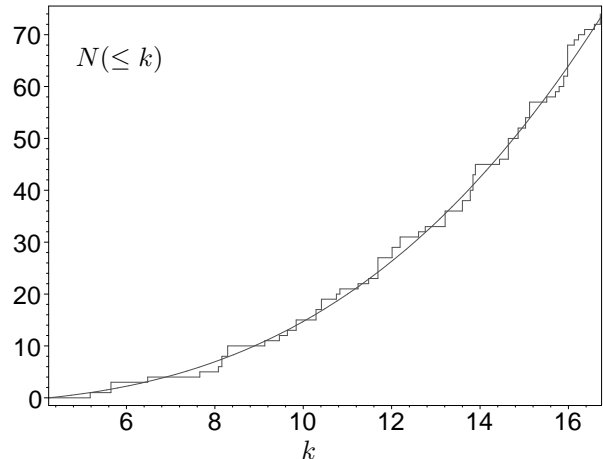


FIG. 3. The spectra staircase for $m003(-3, 1)$ showing its convergence toward the Weyl asymptotic formula.

TABLE III. Eigenvalue spectrum for the Weeks space.

27.8	32.9	43.0	59.7	66.3	67.6
1	2	1	1	1	2
69.7	84.4	90.5	93.9	97.8	106.9
2	1	1	1	2	2
109.4	116.6	118.3	127.3	132.8	137.7
2	1	1	1	1	4
145.2	149.6	160.0	163.8	175.5	186.0
2	2	1	1	3	2
190.9	192.6	194.1	209.5	215.3	221.8
2	3	2	1	4	2
226.9	229.6	241.6	247.6	250.3	253.6
2	3	1	1	1	2
256.4	261.2	264.3	268.8	276.2	280.6
6	1	1	1	1	2

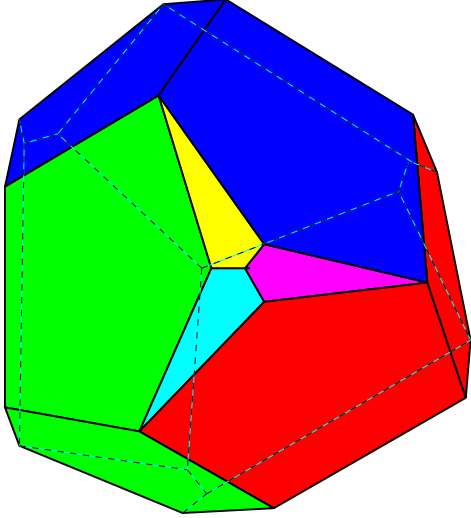


FIG. 4. A Dirichlet domain for the Weeks space shown in Klein coordinates. Like-colored sides of the polyhedron are topologically identified.

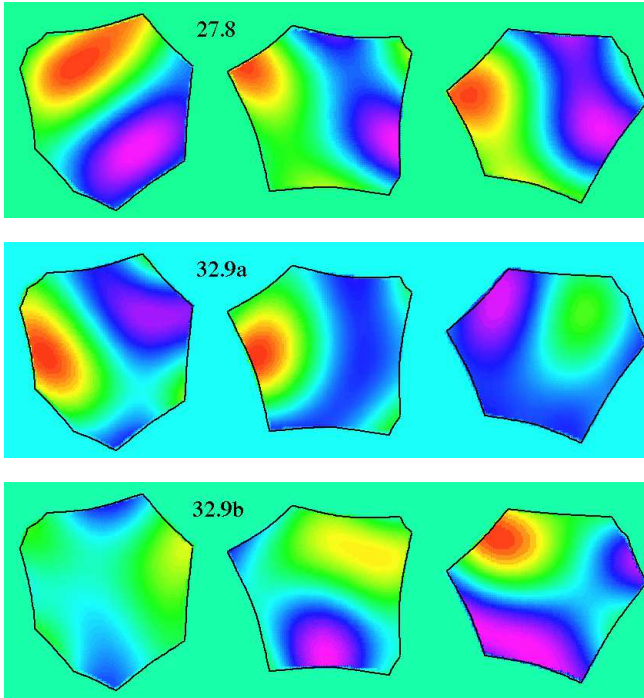


FIG. 5. The first three eigenmodes of the Weeks space. The three views in each panel are, respectively, the $x = 0$, $y = 0$ and $z = 0$ slices through the fundamental domain. Here we are using Poincaré coordinates.

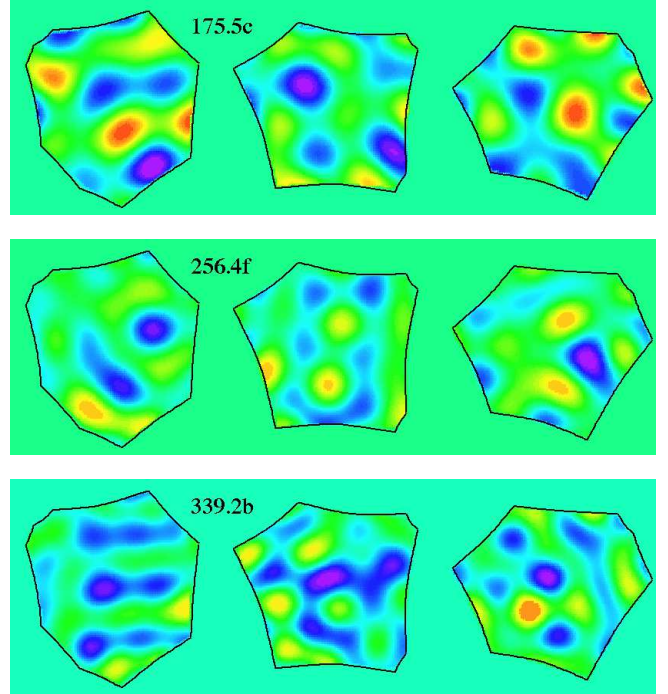


FIG. 6. The first of the 3 and 6 fold degenerate modes of the Weeks space. Also shown is the highest mode we generated.

B. The GOE Prediction

Compact hyperbolic manifolds provide the archetypal setting for chaos. Consequently, we expect the statistical properties of the modes to be described by random matrix theory [11]. Because the modes are associated with time-reversal invariant dynamics, we expect the statistical properties to be those of a Gaussian Orthogonal Ensemble (GOE). The GOE prediction is that the quantity

$$x = \frac{|a_{k\ell m} - \bar{a}_k|^2}{\sigma_k^2}, \quad (3.3)$$

should behave as a pseudo-random number with probability distribution

$$P(x) = \frac{1}{\sqrt{2\pi x}} e^{-x/2}. \quad (3.4)$$

In the above equations, \bar{a}_k denotes the average of the $a_{k\ell m}$'s and σ_k^2 their variance. To avoid the singularity at $x = 0$, it is conventional to compare numerical results to the cumulative distribution

$$I(x) = \int_0^x P(x) dx = \text{erf}(\sqrt{x/2}). \quad (3.5)$$

Taking the mode with eigenvalue $q^2 = 175.5$ as an example, we display in Fig. 7 the first 676 $a_{k\ell m}$'s in a

scatter plot. Notice that the distribution is independent of ℓ and m , as expected for a chaotically mixed state.

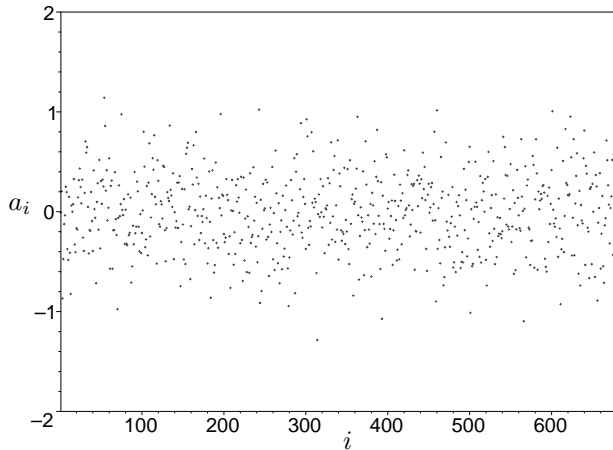


FIG. 7. The $a_{k\ell m}$'s for the eigenmode $q^2 = 175.5$, shown up to $\ell_{\max} = 25$. The numbering scheme for the modes maps $a_{\ell m} \mapsto a_i$ where $i = \ell^2 + \ell + 1 + m$.

The cumulative distribution $I(x)$ is compared to the GOE prediction in Fig. 8. The agreement is quite remarkable.

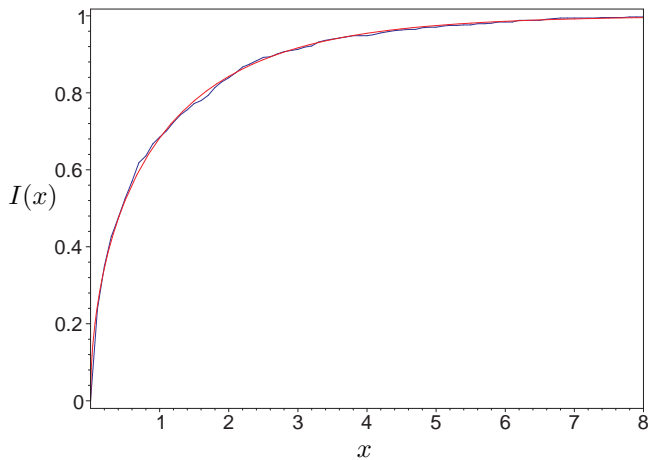


FIG. 8. The cumulative distribution $I(x)$ found for the eigenmode with $q^2 = 175.5$ (blue line) and the GOE prediction (red line).

C. The circles test

The next test we applied to the modes is one that we plan to apply to our own universe [5,6,12]. Imagine drawing a 2-sphere of radius ρ about the basepoint of the Dirichlet domain. Viewed in the universal cover, the space will contain an infinite number of copies of this

2-sphere. If the radius of the 2-sphere exceeds the in-radius of the Dirichlet domain, then the 2-spheres will intersect along a circle. Mapping the entire picture back inside the Dirichlet domain, we see that the 2-sphere self-intersects. If we now take a 2-sphere slice through one of the eigenmodes, the amplitude of the mode must match up around the matched pair of circles.

The largest matched circles lie on face-planes of the Dirichlet domain. Taking a face-pairing generator g , and representing it as a 4×4 real matrix in $SO(3,1)$, the angular radius α of the matched circle is

$$\alpha = \arccos \left(\frac{g_{00} - 1}{\sqrt{g_{00}^2 - 1} \tanh(\rho)} \right). \quad (3.6)$$

The (θ, ϕ) coordinates of the circle centers are

$$\left(\arccos \left(g_{10} / \sqrt{g_{00}^2 - 1} \right), \arctan (g_{30} / g_{20}) \right), \\ \left(\arccos \left(g_{10}^{-1} / \sqrt{g_{00}^2 - 1} \right), \arctan (g_{30}^{-1} / g_{20}^{-1}) \right). \quad (3.7)$$

We display in Fig. 9 the amplitude of the eigenmodes $q^2 = 43.0$ and $q^2 = 84.4$ around a 2-sphere of radius $\rho = 1$ using an equal-area projection. Two of the matched circle pairs are indicated by white lines. In Fig. 10 we plot the amplitude of each mode around each pair of circles and see that they are indeed properly matched. If our universe is multi-connected, we hope to see similar matched circles in the cosmic microwave sky [5,6].

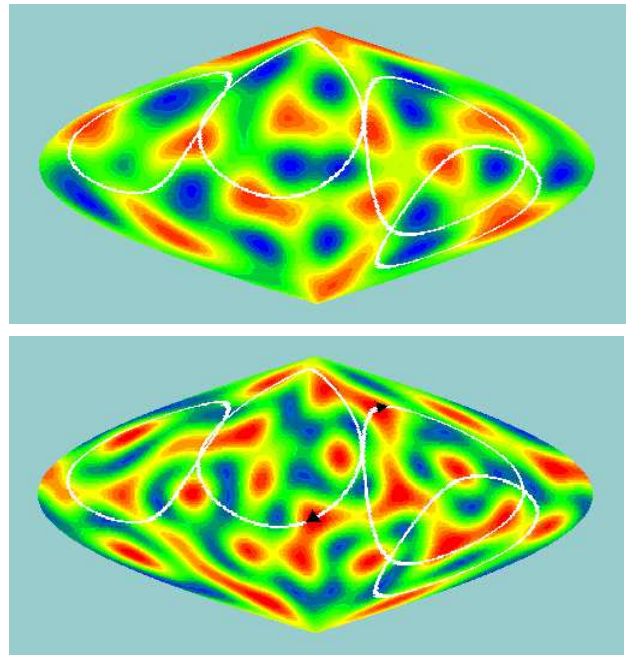


FIG. 9. A two-dimensional slice through the $q^2 = 43.0$ (upper panel) and $q^2 = 84.4$ (lower panel) eigenmodes. The slice is taken on a 2-sphere of unit radius. Two pairs of matched circles are also indicated. The relative phasing of one matched pair is shown on the lower panel.

IV. THE LOWEST EIGENMODES

Having established that our algorithm is reliable, we set it loose on the *SnapPea* census to produce the list of lowest eigenvalues recorded in Table IV. The lowest eigenvalue, q_1^2 , is a useful topological invariant that has attracted considerable attention in the mathematical literature. There exist a variety of upper and lower bounds on q_1^2 . A summary of these bounds can be found in the works of Callahan [13] and Cornish *et al.* [14]. Amongst the sharpest are those that employ the diameter[†], D , of the space:

$$\frac{4\tilde{D}}{D^2(\sinh(\tilde{D}) + \tilde{D})^2} \leq q_1^2 \leq 1 + \left(\frac{2\pi}{D}\right)^2. \quad (4.1)$$

Here \tilde{D} denotes the square root of the smallest integer that is greater than or equal to D^2 . A listing of the diameters can be found in Table V. In all cases, the lowest eigenvalues found by our algorithm fell in the range dictated by (4.1). The eigenvalue bound (4.1) tells us that the wavelength of the lowest eigenmode must be greater than or equal to the diameter of the space. Curiously, we found that $\lambda_1 = (1.3 \rightarrow 1.6)D$ for all twelve examples studied.

On a cautionary note, the eigenvalues listed in Table IV might not be the lowest supported by these spaces. Our method for finding the eigenmodes is unable to detect modes with $q^2 < 1$, as these modes have imaginary wavenumbers. Moreover, the spherical eigenmodes we use as our expansion basis start to look very much alike for wavenumbers $k < 1$, so we may have missed modes in the range $k = [0, 1/4]$. We are currently developing a variant of our method to handle all modes below $q^2 = 2$. At the other end of the spectrum, the only limitation in going out to $q^2 = \infty$ is computer power. To get all the

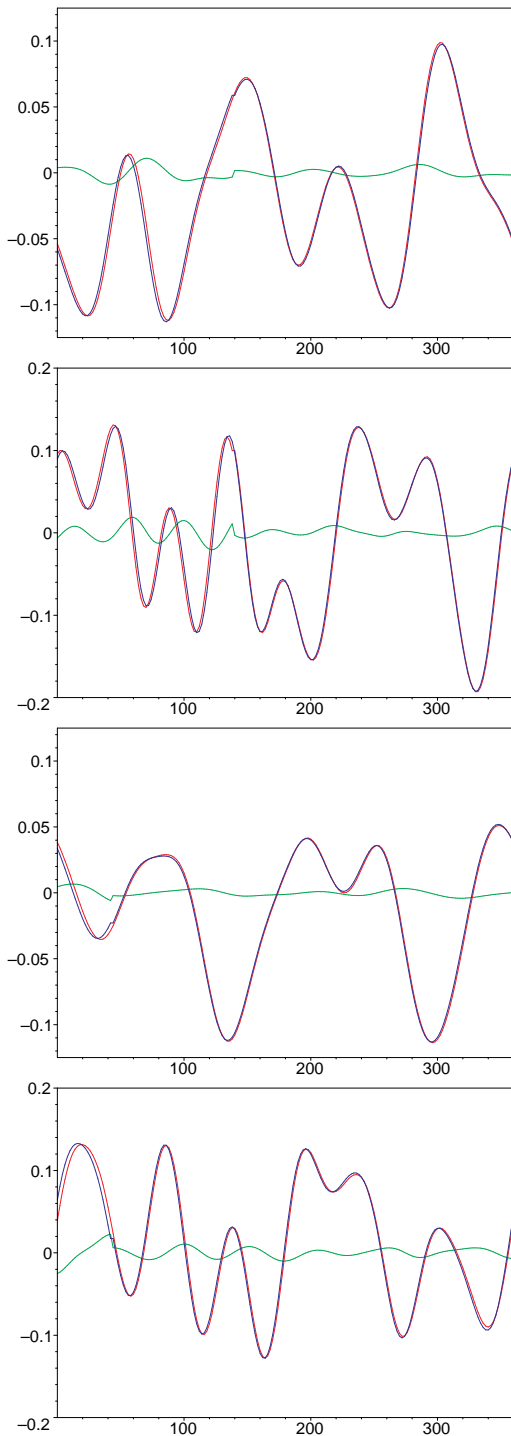


FIG. 10. Each panel shows Ψ_q around a pair of matched circles, C (in red) and \tilde{C} (in blue). Also shown (in green) is the difference $\Psi_q - \tilde{\Psi}_q$ around the matched pair. This small difference represent the numerical error in our algorithm. The first panel correspond to the mode $q^2 = 43.0$ sampled along the inner pair of circles. The second panel shows the same pair of circles, but for the mode $q^2 = 84.4$. The third and fourth panels are likewise shown for the outer pair of circles.

TABLE IV. Lowest eigenvalues

Σ	Vol	G	q_1^2	m_1
m003(-3,1)	0.9427	D_6	27.8	1
m003(-2,3)	0.9814	D_2	29.3	1
s556(-1,1)	1.0156	Z_4	27.9	1
m006(-1,2)	1.2637	D_4	21.1	2
m188(-1,1)	1.2845	D_2	20.4	1
v2030(1,1)	1.3956	D_2	16.2	1
m015(4,1)	1.4124	D_2	28.1	2
s718(1,1)	2.2726	D_2	10.1	1
m120(-6,1)	3.1411	Z_2	7.50	1
s654(-3,1)	4.0855	D_2	5.88	1
v2833(2,3)	5.0629	Z_2	6.29	1
v3509(4,3)	6.2392	D_2	6.06	1

[†]The diameter is defined to equal the greatest distance between any two points in the manifold.

TABLE V. L_γ , diameter, wavelength and wavenumber

Σ	L_γ	D	λ_1/D	k_1
m003(-3,1)	0.585	0.843	1.44	5.18
m003(-2,3)	0.578	0.868	1.36	5.32
s556(-1,1)	0.831	0.833	1.45	5.19
m006(-1,2)	0.575	1.017	1.38	4.48
m188(-1,1)	0.480	0.995	1.44	4.41
v2030(1,1)	0.366	1.082	1.49	3.90
m015(4,1)	0.794	0.923	1.31	5.21
s718(1,1)	0.339	1.439	1.45	3.01
m120(-6,1)	0.314	1.694	1.45	2.55
s654(-3,1)	0.312	1.946	1.46	2.21
v2833(2,3)	0.486	1.701	1.60	2.30
v3509(4,3)	0.346	1.802	1.55	2.25

modes out to $q^2 = 250$ takes around 12 hours on a single R1000 Silicon Graphics chip (or 10 minutes if you use a 64 processor Origin 2000 supercomputer as we did).

V. ACKNOWLEDGMENTS

We are indebted to Ralf Aurich, Craig Hodgson and Jeff Weeks for answering our many questions about the structure of the eigenmodes, the properties of the symmetry groups and the topology of 3-manifolds. We are grateful for the support provided by NASA through their funding of the MAP satellite mission <http://map.gsfc.nasa.gov/>.

-
- [1] G.D. Mostow, Ann. Math. Studies **78** (Princeton University Press, Princeton, 1973); G. Prasad, Invent. Math. **21**, 255 (1973).
 - [2] M. Kac, Amer. Math. Monthly **73**, 1, (1966).
 - [3] R. Aurich and F. Steiner, Physica D**48**, 445 (1991).
 - [4] R. Aurich and F. Steiner, Physica D**64**, 185 (1993).
 - [5] N.J. Cornish, D. Spergel & G. Starkman, Phys. Rev. Lett. **77**, 215 (1996).
 - [6] N.J. Cornish, D. Spergel & G. Starkman, Class. Quant. Grav. **15**, 2657 (1998).
 - [7] R. Aurich and J. Marklof, Physica D**92**, 101 (1996).
 - [8] K. Inoue, astro-ph/9810034, (1998).
 - [9] W.H. Press *et al.*, *Numerical Recipes: The art of scientific computing*, (Cambridge University Press, Cambridge, 1992)
 - [10] J. Weeks, *SnapPea*: A computer program for creating and studying hyperbolic 3-manifolds, available at <http://www.geom.umn.edu:80/software>.
 - [11] M. L. Mehta, *Matrices and the Statistical Theory of Energy Levels*, (Academic Press, New York, 1967).
 - [12] J. Weeks, Class. Quant. Grav. **15**, 2599 (1998).
 - [13] P. Callahan, *Ph.D. Thesis, Univ. of Texas*.
 - [14] N.J. Cornish, D. Spergel & G. Starkman, Phys. Rev. D**57**, 5982 (1998).